

AtNFXL1, an Arabidopsis homologue of the human transcription factor NF-X1, functions as a negative regulator of the trichothecene phytotoxin-induced defense response

著者	Asano Tomoya, Masuda Daisuke, Yasuda Michiko, Nakashita Hideo, Kudo Toshiaki, Kimura Makoto, Yamaguchi Kazuo, Nishiuchi Takumi
journal or publication title	Plant Journal
volume	53
number	3
page range	450-464
year	2008-02-01
URL	http://hdl.handle.net/2297/9895

doi: 10.1111/j.1365-313X.2007.03353.x

the plant journal

***AtNFXL1*, an *Arabidopsis* homologue of the human transcription factor NF-X1, functions as a negative regulator of the trichothecene phytotoxin-induced defense response.**

Journal:	<i>The Plant Journal</i>
Manuscript ID:	TPJ-00751-2007.R1
Manuscript Type:	Full Paper
Date Submitted by the Author:	n/a
Complete List of Authors:	Asano, Tomoya; Kanazawa University, Advanced Science Research Center Masuda, Daisuke; Kanazawa University, ASRC Yasuda, Michiko; RIKEN, Environmental Molecular Biology Laboratory Nakashita, Hideo; RIKEN, Environmental Molecular Biology Laboratory Kudo, Toshiaki; RIKEN, Environmental Molecular Biology Laboratory Kimura, Makoto; RIKEN, Discovery Research Institute (DRI), Plant & Microbial Metabolic Engineering Research Unit Yamaguchi, Kazuo; Kanazawa University, ASRC Nishiuchi, Takumi; Kanazawa university, ASRC
Key Words:	trichothecene, phytotoxin, microarray, transcription factor, Fusarium, defense response, SA biosynthesis



1
2
3
4
5
6
7 ***AtNFXL1*, an *Arabidopsis* homologue of the human transcription factor NF-X1,**
8
9
10 **functions as a negative regulator of the trichothecene phytotoxin-induced defense**
11
12
13
14 **response.**

15
16
17 Tomoya Asano^{1, 2}, Daisuke Masuda¹, Michiko Yasuda³, Hideo Nakashita³, Toshiaki
18
19
20 Kudo³, Makoto Kimura⁴, Kazuo Yamaguchi^{1, 5} and *Takumi Nishiuchi^{1, 5}
21
22

23
24 ¹Division of Functional Genomics, Advanced Science Research Center, Kanazawa
25
26
27 University, 13-1 Takaramachi, Kanazawa 920-0934, Japan; ²Shigeta Animal
28
29
30 Pharmaceuticals Inc., 4569-1, Komoridani, Oyabe City, Toyama Prefecture, 932-0133
31
32
33
34 Japan; ³Environmental Molecular Biology Laboratory, RIKEN, 2-1 Hirosawa, Wako,
35
36
37 Saitama 351-0198, Japan; ⁴Plant & Microbial Metabolic Engineering Research Unit,
38
39
40
41 Discovery Research Institute (DRI), RIKEN, 2-1 Hirosawa, Wako, Saitama 351-0198, Japan;
42
43
44
45 ⁵Division of Life Science, Graduate School of Natural Science and Technology,
46
47
48 Kanazawa University, Kanazawa 920-1192, Japan
49

50
51 *Author for correspondence (e-mail: tnish9@kenroku.kanazawa-u.ac.jp)
52
53
54
55
56
57

58 total word count: **7,134**
59
60

1
2
3
4
5
6
7 Running title: Trichothecene-inducible *AtNFXL1* gene
8
9

10 key words: phytotoxin, trichothecene, transcription factor, defense response
11
12
13
14
15
16
17
18
19
20
21
22
23
24
25
26
27
28
29
30
31
32
33
34
35
36
37
38
39
40
41
42
43
44
45
46
47
48
49
50
51
52
53
54
55
56
57
58
59
60

CONFIDENTIAL

Abstract

Trichothecenes are a closely related family of phytotoxins produced by phytopathogenic fungi. In *Arabidopsis*, expression of *AtNFXL1*, a homologue of the putative human transcription repressor *NF-X1*, was significantly induced by application of type A trichothecenes, such as T-2 toxin. An *atnfxl1* mutant growing on medium lacking trichothecenes showed no phenotype, whereas a hypersensitivity phenotype was observed in T-2 toxin-treated *atnfxl1* mutant plants. Microarray analysis indicated that several defense-related genes (i.e. *WRKYs*, *NBS-LRRs*, *EDS5*, *ICSI*, etc.) were upregulated in T-2 toxin-treated *atnfxl1* mutant compared to wild type plants. In addition, enhanced salicylic acid (SA) accumulation was observed in T-2 toxin-treated *atnfxl1* mutant plants, which suggests that *AtNFXL1* functions as a negative regulator of these defense-related genes via an SA-dependent signaling pathway. We also found that expression of *AtNFXL1* was induced by SA and flg22 treatment. Moreover, the *atnfxl1* mutant was less susceptible to a compatible phytopathogen, *Pseudomonas syringae* pv. tomato strain DC3000 (*Pst* DC3000). Taken together, these results indicate

1
2
3
4
5
6
7 that *AtNFXL1* plays an important role in the trichothecene response, as well as the

8
9
10 general defense response in *Arabidopsis*.
11
12
13
14
15
16
17
18
19
20
21
22
23
24
25
26
27
28
29
30
31
32
33
34
35
36
37
38
39
40
41
42
43
44
45
46
47
48
49
50
51
52
53
54
55
56
57
58
59
60

CONFIDENTIAL

Introduction

Trichothecenes are a major type of mycotoxin, and are important in human health due to the risk of ingesting contaminated food (Kimura *et al.*, 2006). Phytopathogenic fungi capable of producing trichothecenes are found throughout the world, and include certain species of *Fusarium*, *Myrotherium* and *Stachybotrys* (Eudes *et al.*, 2001). The production of mycotoxins by these species of phytopathogenic fungi is determined by genetic factors and environmental growth conditions. Trichothecenes have a sesquiterpenoid ring structure, and can be classified according to the presence or absence of characteristic functional groups (Shifrin and Anderson, 1999). Type A trichothecenes, such as T-2 toxin, and type B trichothecenes, such as deoxynivalenol (DON), are natural contaminants of certain agricultural commodities, as well as commercial foods (Sudakin, 2003). Among the trichothecenes, type A trichothecenes are highly toxic at low concentrations.

Trichothecenes inhibit peptidyltransferase activity in eukaryotic cells by binding to the 60S ribosomal subunit. The antiproliferative activity of trichothecenes is presumed to be a consequence of their ability to inhibit protein synthesis (Shifrin and

1
2
3
4
5
6
7 Anderson, 1999). Thus, trichothecenes also function as phytotoxins. Specific disruption
8
9
10 of a trichothecene synthase gene (*Tri5*) in *F. graminearum* resulted in a strain that was
11
12
13 less virulent in the infection of wheat compared to wild type strains (Desjardins *et al.*,
14
15
16 2000). For this reason, Desjardins *et al.* have suggested that in certain *Fusarium* species,
17
18
19 trichothecenes act as virulence factors in the infection of plants (Desjardins *et al.*, 2000).
20
21
22 Trichothecene-producing *Fusarium* species have strain-specific trichothecene
23
24
25 metabolite profiles (Ward *et al.*, 2002), and these trichothecene chemotypes are also
26
27
28
29
30
31 believed to play a role in the virulence of individual strains of *Fusarium*.
32
33

34
35 Recently, we reported that type A trichothecenes, such as T-2 toxin, have an
36
37
38 elicitor-like activity in *Arabidopsis thaliana* at a concentration of 1 μM (Nishiuchi *et al.*,
39
40
41 2006). Type A trichothecene-inducible lesions were also formed in SA-, jasmonic acid
42
43
44 (JA)- and ethylene (ET)-mutants, and in SA-deficient *NahG* transgenic plants
45
46
47 (Nishiuchi *et al.*, 2006). These results implied that T-2 toxin-induced cell death has little
48
49
50
51 to do with these host defense pathways; rather, the toxin contributes directly to the
52
53
54 virulence of necrotrophic phytopathogens. In contrast to T-2 toxin, 10 μM DON
55
56
57 inhibited protein translation in *Arabidopsis* cells, whereas it failed to activate the
58
59
60

1
2
3
4
5
6
7 elicitor-like signaling pathway (Nishiuchi *et al.*, 2006), which suggests that *Fusarium*
8
9
10 utilizes DON as a non-defense-inducing translational inhibitor during the spread of
11
12
13 disease in host plants (Bai *et al.*, 2001). Thus, the role of type B trichothecenes in
14
15
16 virulence might be different from that of type A trichothecenes. Urban *et al.* reported
17
18
19 that the DON-producing, wheat-attacking fungal pathogens *F. graminearum* and *F.*
20
21
22 *culmorum* can infect the flowers of *Arabidopsis* contaminated with DON (Urban *et al.*,
23
24
25
26
27
28
29
30
31
32
33
34
35
36
37
38
39
40
41
42
43
44
45
46
47
48
49
50
51
52
53
54
55
56
57
58
59
60
2002).

We recently reported that *AtNFXL1* is upregulated in T-2 toxin-treated *Arabidopsis* (Masuda *et al.*, 2007). *AtNFXL1* encodes a putative transcription factor with similarity to the human transcription repressor NF-X1 (Lisso *et al.*, 2006). Human NF-X1 was identified as a binding factor for the conserved X1 box regulatory element in the proximal promoters of class II *MHC* genes, and contains a nuclear localization signal (NLS), a RING-CH finger domain, several NF-X1-type zinc (Zn) finger domains, and an R3H domain (Song *et al.*, 1994). Song *et al.* suggested that NF-X1 is involved in regulating disease states by suppressing the expression of class II *MHC* genes (Song *et al.*, 1994). The RING-CH finger domain is implicated in the targeting of proteins for

1
2
3
4
5
6
7 ubiquitination (Lorick *et al.*, 1999). The yeast *NF-X1* homologue, *FAP1*, was identified
8
9
10 in a genetic screen for suppressors of rapamycin toxicity (Kunz *et al.*, 2000). *FAP1*
11
12
13 interacted physically with a FK506-binding protein 12 (FKBP12) *in vivo* and *in vitro*,
14
15
16
17 and suppressed the cytotoxic effects of rapamycin (Kunz *et al.*, 2000). Strombakis *et al.*
18
19
20 suggested that the *Drosophila NF-X1* homologue, *shuttle craft (stc)*, is essential for
21
22
23 embryogenesis by regulating the activity of a subset of genes that play a role in either
24
25
26 the guidance or spatial maintenance of axon tracts (Strombakis *et al.*, 1996). Taken
27
28
29 together, these results suggest that the NF-X1 family of proteins has unique functions in
30
31
32 different organisms.
33
34
35

36
37 In this paper, we demonstrated that *atnfxl1* mutant plants exhibit a hypersensitivity
38
39
40 phenotype to a type A trichothecene, T-2 toxin. Microarray analysis revealed that many
41
42
43 defense-related genes are upregulated in the *atnfxl1* mutant in the presence of
44
45
46 trichothecenes, compared to wild type plants. High levels of SA accumulated in T-2
47
48
49 toxin-treated *atnfxl1* mutant plants compared to wild type plants, which suggests that
50
51
52 *AtNFXL1* functions as a negative regulator of defense-related genes via an
53
54
55 SA-dependent signaling pathway. In addition, we found that the expression of *AtNFXL1*
56
57
58
59
60

1
2
3
4
5
6
7 is induced by application of SA. Moreover, the *atnfxl1* mutant was less susceptible to
8
9
10 the compatible phytopathogen *Pst* DC3000. Thus, *AtNFXL1* also appears to play an
11
12
13 important role in the defense response to compatible phytopathogens in *Arabidopsis*.
14
15
16
17
18
19

20 **Results**

21 **AtNFXL1 belongs to the NF-X1 family of proteins**

22
23
24 Based on its predicted amino acid sequence, *AtNFXL1* encoded a protein with a
25
26
27 molecular weight of 130 kDa that has similarity to the human transcription repressor
28
29
30 NF-X1 (Supplemental Figures 1a and b). *AtNFXL1* contains several functional regions
31
32
33 and domains, including an NLS, a RING-CH finger domain, and nine NF-X1-type Zn
34
35
36 finger domains (Supplemental Figure 1a). These domains are also conserved in *Oryza*
37
38
39 *sativa* OsNF-X1, *Homo sapiens* NF-X1, *Drosophila melanogaster* STC, and
40
41
42 *Saccharomyces cerevisiae* FAP1. The R3H domain, which is involved in binding of
43
44
45 single stranded RNA, is present only in NF-X1 family proteins of non-plant eukaryotes
46
47
48 (Supplemental Figure 1a). Phylogenetic analysis indicated that plant NF-X1-like
49
50
51 proteins are more closely related to human NF-X1 than to FAP1 or STC (Supplemental
52
53
54
55
56
57
58
59
60

1
2
3
4
5
6
7 Figure 1b). *AtNFXL1* contains an intron in its 5'UTR (data not shown). The NF-X1-type
8
9
10 Zn finger domains are unique motifs, and the Zn finger repeats are conserved in
11
12
13 *AtNFXL1* (Supplemental Figure 1c) . It has been reported that a green fluorescent
14
15
16 protein (GFP)-*AtNFXL1* fusion protein localizes to the nucleus in onion epidermal cells
17
18
19 (Lisso et al., 2006). We also examined the localization of a GFP-*AtNFXL1* fusion
20
21
22 protein in *Arabidopsis*, and found that GFP-*AtNFXL1* localizes to the nucleus in
23
24
25
26
27 *Arabidopsis* T87 suspension cultured cells (Supplemental Figure 2).
28
29
30
31
32
33

34 **The *atnfxl1* mutant displays a hypersensitivity phenotype to the type A**
35
36
37 **trichothecene, T-2 toxin.**
38
39

40
41 We recently demonstrated that *AtNFXL1* is a trichothecene-inducible gene (Masuda *et*
42
43
44 *al.*, 2007). To determine the function of *AtNFXL1*, we investigated the trichothecene
45
46
47 response of *atnfxl1* (*atnfxl1-1*) mutant plants. The *atnfxl1-1* mutant was generated by
48
49
50 transferred-DNA (T-DNA) insertion at position +2,082 (relative to the first basepair of
51
52
53 the initiation codon at +1) of the open reading frame of *AtNFXL1* (Munich Information
54
55
56
57
58 Center for Protein Sequence designation At1g10170), as previously described (Figure
59
60

1
2
3
4
5
6
7 1a; Lisso *et al.*, 2007). In wild type plants, *AtNFXL1* was weakly expressed in the
8
9
10 absence of T-2 toxin, whereas it was induced by 1 μ M T-2 toxin treatment, as previously
11
12 reported (Figure 1b; Masuda *et al.*, 2007). In the *atnfxl1* mutant, we observed a
13
14 truncated transcript of *AtNFXL1* (Figure 1b). The deduced amino acid sequence of the
15
16 truncated mRNA in the *atnfxl1* mutant lacked two of the nine NF-X1-type Zn finger
17
18 domains. Therefore, it is likely that the truncated form of *atnfxl1* mRNA in mutant
19
20 plants does not encode a functional protein. The *atnfxl1* mutant exhibited no apparent
21
22 phenotype on MS agar medium alone (without trichothecene) compared to wild type
23
24 plants (Figures 1c and 1d). In addition, general phenotypes, such as growth rate, organ
25
26 development, and morphology of untreated *atnfxl1* mutant were similar to wild type
27
28 plants (data not shown). In contrast, *atnfxl1* mutant exhibited a severe growth defect on
29
30 MS medium containing 0.1 μ M T-2 toxin (Figures 1c and 1d). As previously reported
31
32 (Masuda *et al.*, 2007), cell death was not induced when seedlings were transferred to
33
34 0.1-1 μ M T-2 toxin-containing medium. The T2 segregation ratio of the
35
36 toxin-hypersensitivity phenotype was nearly 1:3 in self-pollinated offspring of
37
38 heterozygous *atnfxl1* plants, which indicated that the mutation was inherited as a single
39
40
41
42
43
44
45
46
47
48
49
50
51
52
53
54
55
56
57
58
59
60

1
2
3
4
5
6
7 recessive trait. As shown in Figure 1d, the growth defects of DON-treated *atnfxl1*
8
9
10 mutant were similar to DON-treated wild type plants.
11

12
13 To determine whether the T-2 toxin-sensitive phenotype of *atnfxl1* mutant
14
15
16
17 plants was due to a defect in *AtNFXL1*, we carried out a complementation analysis.
18
19
20 Introduction of a complementation plasmid containing the promoter and the coding
21
22
23 sequence of *AtNFXL1* (*AtNFXL1 promoter::AtNFXL1*, see Experimental Procedures)
24
25
26
27 into *atnfxl1* mutant plants clearly rescued the hypersensitivity phenotype in the presence
28
29
30 of 0.1 μ M T-2 toxin in 7 of 8 plant lines (Figures 1c and 1d). These results demonstrated
31
32
33 that the hypersensitivity to T-2 toxin of *atnfxl1* mutant plants was due to a defect in
34
35
36
37 *AtNFXL1*.
38
39
40
41
42
43
44

45 **Defense-related genes are upregulated in trichothecene-treated *atnfxl1* mutant**
46
47
48 **plants.**
49

50
51 We performed a transcriptome analysis of approximately 14,880 genes to obtain the
52
53
54 expression profiles of putative *AtNFXL1*-regulated genes. This analysis was carried out
55
56
57
58 using two independent wild-type plants, and two independent mutant plant lines. As
59
60

1
2
3
4
5
6
7 seen in Figure 1b, *atnfxl1* mutant plants displayed no visible phenotype in the absence
8
9
10 of trichothecenes. In accordance with this result, none of the genes we examined were
11
12
13 upregulated more than 3-fold in *atnfxl1* mutant plants compared to wild type plants in
14
15
16 the absence of trichothecenes (data not shown). A single gene was down-regulated
17
18
19 greater than 3-fold in *atnfxl1* mutant plants compared to wild type plants (data not
20
21
22 shown). These results indicated that in the absence of trichothecenes, *AtNFXL1* has a
23
24
25 minor effect on the global regulation of gene expression.
26
27
28
29
30

31 In contrast, in 1 μ M T-2 toxin-treated *atnfxl1* mutant plants, 130 genes were
32
33
34 upregulated greater than 3-fold compared to T-2 toxin-treated wild type plants (Table 1).
35
36
37 As seen in Table 1, 18 of the upregulated genes were putative transcriptional regulators.
38
39
40 In particular, 8 *WRKY* family genes were upregulated in T-2 toxin-treated *atnfxl1* mutant
41
42
43 plants. *WRKY* transcription factors play pivotal roles in the plant defense response
44
45
46 (Eulgem *et al.*, 2000), and expression of some *WRKY* family genes confers enhanced
47
48
49 disease resistance in *Arabidopsis* and tobacco (Asai *et al.*, 2002; Liu *et al.*, 2004; Chen
50
51
52 and Chen, 2002).
53
54
55
56
57

58 The largest category of putative *AtNFXL1*-regulated genes (28 genes) encoded
59
60

1
2
3
4
5
6
7 cellular communication and signal transduction factors (Table 1). This category
8
9
10 included 9 genes that encode serine/threonine protein kinases, including a Pto-like
11
12
13 kinase, and 7 genes that encode receptor-like protein kinases, which suggests that these
14
15
16 genes function as components of *AtNFXL1*-regulated defense signaling pathways.
17
18
19
20 Several defense-related genes also appeared to be regulated by *AtNFXL1*, including 5
21
22
23 genes that encode disease resistance proteins, as well as *EDS5* and *ICS1*. *EDS5* was
24
25
26 identified as an essential component of SA-dependent signaling in resistance to *Pst*
27
28
29
30 DC3000 in *Arabidopsis* (Nawrath *et al.*, 2002). *ICS1* encodes an isochorismate synthase,
31
32
33 and is required for biosynthesis of SA (Wildermuth *et al.*, 2001). These results
34
35
36 suggested that *AtNFXL1* is involved in SA-dependent defense signaling pathways in
37
38
39 trichothecene-treated *Arabidopsis*.
40
41
42

43
44 Table 2 lists the genes that were down-regulated greater than 3-fold in T-2
45
46
47 toxin-treated *atnfxl1* mutant plants compared to wild type plants. The list of genes
48
49
50 included *LHCB2-4*, which suggests that hyperactivation of the defense response affects
51
52
53 the expression of photosynthesis-related genes.
54
55
56

57
58 To validate the results of the microarray analysis, we selected 6 genes that
59
60

1
2
3
4
5
6
7 were upregulated, and 1 gene that was down-regulated in T-2 toxin-treated *atnfxl1*
8
9
10 mutant plants, and analyzed them by real time PCR. As shown in Table 3, we obtained
11
12
13 similar results using real time PCR, although the magnitude of the expression change of
14
15
16
17 some of the genes was greater than what was observed by microarray analysis.
18
19
20

21 22 23 24 **Enhanced SA accumulation in T-2 toxin-treated *atnfxl1* mutant plants.**

25
26
27 Microarray analysis revealed that defense-related genes, including genes involved in SA
28
29
30 biosynthesis, were upregulated in *atnfxl1* mutant compared to wild type plants. *PR-1*
31
32
33 (*At2g14160*), which is regulated in an SA-dependent manner, was not present on the
34
35
36 Agilent *Arabidopsis 1* microarray. When we examined the expression of *PR-1* by
37
38
39 RT-PCR, we found that *PR-1* was weakly induced 24 hours (hr) after T-2 toxin
40
41
42 treatment in both wild type and *atnfxl1* mutant, as previously described (Masuda et al.,
43
44
45 2007). The T-2 toxin-induced expression of *ICS1* was enhanced in *atnfxl1* mutant plants
46
47
48 compared to wild type plants (Figure 2a). These results suggested that SA biosynthesis
49
50
51 is activated in *atnfxl1* mutant plants. We next measured free and total SA levels in wild
52
53
54 type and *atnfxl1* mutant plants in the presence or absence of T-2 toxin. As seen in
55
56
57
58
59
60

1
2
3
4
5
6
7
8
9
10
11
12
13
14
15
16
17
18
19
20
21
22
23
24
25
26
27
28
29
30
31
32
33
34
35
36
37
38
39
40
41
42
43
44
45
46
47
48
49
50
51
52
53
54
55
56
57
58
59
60

Figures 2b and 2c, T-2 toxin-induced SA accumulation was enhanced in *atnfxl1* mutant plants compared to wild type plants. Taken together, these results suggested that enhanced SA accumulation in *atnfxl1* mutant plants leads to the induction of defense-related genes (Table 1).

SA and flg22 activate the transcription of *AtNFXL1*.

To investigate the expression pattern of *AtNFXL1* in more detail, we generated transgenic plants carrying an *AtNFXL1 promoter::β-glucuronidase (GUS)* gene fusion construct. As shown in Figure 3a, in seedlings of *AtNFXL1::GUS* transformants, in the absence of trichothecene, GUS activity was present in the vascular bundle and meristematic tissue. *AtNFXL1* promoter activity was increased up to approximately 18-fold by 0.1 μM T-2 toxin treatment compared to mock (no trichothecene) treatment (Figures 3a, 3b and 3d). Treatment with 2.5 μM DAS induced an 8-fold increase in promoter activity, while treatment with 10 μM DON resulted in a 3-fold induction of promoter activity (Figure 3d). Since *AtNFXL1* is predicted to play a role in defense signaling, including SA-dependent signaling, we also investigated whether other

1
2
3
4
5
6
7 elicitors and defense-related signals affected the expression of *AtNFXL1*. *AtNFXL1*
8
9
10 promoter activity was increased approximately 5-fold by flg22, a peptide elicitor
11
12
13 derived from phytopathogenic bacteria (Figure 3d). SA treatment induced an
14
15
16 approximate 40-fold increase in GUS activity in *AtNFXL1* promoter::*GUS*
17
18
19 transformants (Figure 3a, 3c, and 3d), and 1-aminocyclopropane-1-carboxylic acid
20
21
22 (ACC) and methyl jasmonate (MeJA) induced a 2.5-fold and 3.2-fold increase in
23
24
25 promoter activity, respectively (Figure 3d). These results suggested that *AtNFXL1* plays
26
27
28 a role not only in the action of trichothecenes, but also in the general defense response
29
30
31 of *Arabidopsis*.
32
33
34
35
36
37
38
39
40

41 **The *atnfxl1* mutant is less susceptible to *Pst* DC3000.**

42
43
44 To determine whether *AtNFXL1* is involved in disease resistance to phytopathogens,
45
46
47 wild type and *atnfxl1* mutant plants were inoculated with the compatible pathogen *Pst*
48
49
50 DC3000. As shown in Figure 4a, the growth of *Pst* DC3000 in *atnfxl1* mutant plants
51
52
53 was slower than in wild type plants, which indicated that *atnfxl1* mutant plants are less
54
55
56 susceptible to *Pst* DC3000. The reduced susceptibility to the compatible pathogen *Pst*
57
58
59
60

1
2
3
4
5
6
7 DC3000 was not observed after complementation with wild type *AtNFXL1* (Figure 4b).

8
9
10 These results indicated that the reduced susceptibility phenotype of *atnfxl1* mutant is
11
12 due to a defect in *AtNFXL1*. These results also provided further evidence that *AtNFXL1*
13
14 functions not only in the trichothecene response, but also in the general defense
15
16
17
18
19
20 response in *Arabidopsis*.
21
22
23
24
25
26
27

28 Discussion

29
30 The action of trichothecenes in host plants can not simply be attributed to
31
32 general toxicity, such as inhibition of translation. For example, we previously reported
33
34 that some type A trichothecenes have an elicitor-like activity in infiltrated *Arabidopsis*
35
36 leaves (Nishiuchi *et al.*, 2006). Both DON and DAS preferentially inhibit root
37
38 elongation, whereas T-2 toxin-treated seedlings exhibit dwarfism and aberrant
39
40 morphological changes (Masuda *et al.*, 2007). In contrast, neither feature was observed
41
42
43
44
45
46
47
48
49 in seedlings treated with a general translational inhibitor, cycloheximide (CHX).
50
51
52 These results indicate that the action of trichothecenes in plants differs significantly
53
54
55 according to molecular species, and highlight the importance of examining the site of
56
57
58
59
60

1
2
3
4
5
6
7 action of trichothecenes in host plants. In this study, we demonstrated that *AtNFXL1* is
8
9
10 an important regulator of trichothecene action in *Arabidopsis*. Our results may provide a
11
12
13 key to understanding the molecular mechanism of phytotoxic trichothecenes in host
14
15
16
17 plants.

18
19
20 *AtNFXL1* was upregulated not only by type A trichothecenes, but also SA and
21
22 flagellin (Figure 3). SA, in particular, drastically induced the expression of *AtNFXL1*.
23
24 We identified several putative *AtNFXL1*-regulated genes using microarray analysis,
25
26
27 including many defense-related genes, such as *WRKYs*, *RLKs*, and *NBS-LRRs* (Table 1).
28
29
30 Since these genes are putative regulators of defense signaling pathways in *Arabidopsis*,
31
32
33 it is likely that *AtNFXL1* functions as a component of these pathways, particularly the
34
35
36 SA-dependent signaling pathway. Dong *et al.* reported that many of the *Arabidopsis*
37
38
39 *WRKY* family genes are induced by pathogen-infection and/or SA treatment, including
40
41
42 the putative *AtNFXL1*-regulated *WRKY* genes that we identified in the current study
43
44
45 (Dong *et al.*, 2003). Overexpression of *WRKY6* and *WRKY53* results in a dwarfed
46
47
48 phenotype in transgenic plants (Robatzek and Somssich, 2002; Ulker and Somssich,
49
50
51
52
53
54
55
56
57
58
59
60 2004); thus, upregulation of these two genes in *atnfxl1* mutant plants may contribute to

1
2
3
4
5
6
7 the severe growth defects of these plants in the presence of type A trichothecenes. *EDS5*,
8
9
10 which is an essential component of SA-dependent signaling in resistance to *Pst* DC3000
11
12
13 in *Arabidopsis* (Nawrath *et al.*, 2002), and *ICSI*, which encodes an isochorismate
14
15
16 synthase that is required for biosynthesis of SA (Wildermuth *et al.*, 2001), were also
17
18
19 upregulated in T-2 toxin-treated *atnfxl1* mutant plants. In fact, *AtNFXL1* appeared to be
20
21
22 involved in the negative regulation of SA biosynthesis in response to T-2 toxin (Figures
23
24
25 2b and 2c), and possibly other elicitors and infectious pathogens as well. In this manner,
26
27
28 *AtNFXL1* may act to suppress the hyperactivation of defense responses to elicitors or
29
30
31 pathogens. In support of this hypothesis, *atnfxl1* mutant plants displayed less
32
33
34 susceptibility to the compatible phytopathogen *Pst* DC3000 (Figure 4). The *atnfxl1*
35
36
37 mutant could not repress the defense response induced by type A trichothecenes,
38
39
40 resulting in severe growth defects in trichothecene-treated *Arabidopsis* seedlings. This
41
42
43 phenotype was similar to that of the constitutive defense response mutant *cpr1*
44
45
46 (Bowling *et al.*, 1994).
47
48
49
50
51
52

53
54 Lisso *et al.* reported that *AtNFXL1* is induced by salt stress and osmotic stress,
55
56
57 and that *atnfxl1* mutant plants display reduced survival rates after salt stress compared
58
59
60

1
2
3
4
5
6
7 to wild type plants (Lisso *et al.*, 2006). In addition, certain salt-responsive genes, such
8
9
10 as *COR15A*, *KINI*, and *RAB18*, showed weaker expression levels in *atnfxl1* mutant
11
12
13 under salt stress compared to the wild type plants (Lisso *et al.*, 2006). The expression of
14
15
16
17 *COR15A*, *KINI*, and *RAB18* is also induced by ABA in *Arabidopsis* (Baker *et al.*, 1994;
18
19
20 Kurkela and Franck, 1990; Lang and Palva, 1992). In contrast, transgenic
21
22
23
24 *35S::AtNFXL1* plants exhibited an enhanced survival rate under salt stress, and higher
25
26
27 expression of salt-responsive genes. These results indicate that AtNFXL1 functions as a
28
29
30 positive regulator of expression of salt-inducible genes under salt stress conditions
31
32
33
34 (Figure 5). We demonstrated that AtNFXL1 negatively regulates the expression of
35
36
37 several defense-related genes in trichothecene-treated *Arabidopsis* plants (Figure 5).
38
39
40
41 Thus, it seems likely that AtNFXL1 has opposing functions in the salt stress response
42
43
44 and defense response. ABA plays a negative role in defense signaling pathways,
45
46
47 including SA-, JA-, and ET-dependent signaling pathways (Mauch-Mani and Mauch,
48
49
50
51 2005). Therefore, AtNFXL1-controlled stress signaling might depend on components of
52
53
54
55 both the defense and the ABA signaling pathways.

56
57
58 Human NF-X1 binds directly to *cis*-elements in target genes *in vitro*, and
59
60

1
2
3
4
5
6
7 regulates transcription through these elements *in vivo* (Song *et al.*, 1994; Gewin *et al.*,
8
9
10 2004). However, activation or repression domains have not been identified in any
11
12
13 NF-X1 family protein to date. AtNFXL1 contains a RING-CH finger domain, which is
14
15
16
17 a binding motif for the ubiquitin-conjugating enzyme E2s (Lorick *et al.*, 1999). Thus,
18
19
20 AtNFXL1 may function as a repressor by mediating the degradation of its binding
21
22
23 partners. NF-X1 exists as two isoforms: NFX1-123 and NFX1-91. Recently it was
24
25
26
27 shown that NFX1-123 and c-Myc function cooperatively to activate the *hTERT*
28
29
30 promoter, whereas NFX1-91 repressed *hTERT* promoter activity (Gewin *et al.*, 2004).
31
32
33
34 These results raise the possibility that NF-X1 family proteins function as negative
35
36
37 regulators of their targets. In support of this hypothesis, Lisso *et al.* reported that
38
39
40 another *Arabidopsis* NF-X1-like protein, AtNFXL2, is a negative regulator of the salt
41
42
43 stress response (Lisso *et al.* 2006). It has been reported that some elicitor-responsive
44
45
46 RING-H2 finger proteins have roles in plant defense signaling pathways (Takai *et al.*,
47
48
49 2002; Serrano and Guzman, 2004). Thus, the RING-CH finger domain of AtNFXL1
50
51
52 may have a role in regulating the stability of defense-related target proteins.
53
54
55

56
57
58 NF-X1 represses INF- γ -inducible expression of class II *MHC* genes in
59
60

1
2
3
4
5
6
7 INF- γ -treated cells, whereas it has no effect on the expression of these genes in
8
9
10 untreated cells (Song *et al.* 1994). In addition, *FAP1* was identified as a suppressor of
11
12 rapamycin toxicity. *FAP1* physically interacts with FKBP12 *in vivo* and *in vitro* to
13
14 suppress the function of rapamycin, and *FAP1* is targeted to the nucleus by rapamycin
15
16
17 treatment. In the current study, we showed that *atnfxl1* mutant plants are hypersensitive
18
19
20 to the type A trichothecene, T-2 toxin (Figure 2), but display no phenotype in the
21
22
23 absence of chemical. Taken together, these results suggest that *AtNFXL1*, *NF-X1*, and
24
25
26
27 *FAP1* are together involved responding to chemical stimuli, but have no apparent
28
29
30
31
32
33
34
35
36
37
38
39
40
41
42
43
44
45
46
47
48
49
50
51
52
53
54
55
56
57
58
59
60
phenotype in the absence of chemicals.

In summary, we have presented evidence that the trichothecene-inducible gene *AtNFXL1* negatively regulates many defense-related genes, at least in part through the regulation of SA biosynthesis (Figure 5). Additional studies that investigate how *atnfxl1* mutant behave when challenged by necrotrophic pathogens, such as trichothecene-producing fungi, are needed. While we have not established a *Fusarium-Arabidopsis* pathosystem for interaction studies, it has been reported that *A. thaliana* is susceptible to type B DON-producing species of *Fusarium* (Uraban *et al.*,

1
2
3
4
5
6
7 2002). Studies to determine whether *Arabidopsis* is susceptible to T-2 toxin-producing
8
9
10 fungi such as *Fusarium spoichiomerdes* are ongoing, and will further our understanding
11
12
13 of the role of *AtNFXL1* in host plant resistance to trichothecene-producing fungi.
14
15
16
17
18
19
20
21
22
23

24 **Experimental procedures**

25 26 27 **Plant growth and trichothecene treatment**

28
29
30 The Columbia (Col-0) ecotype of *Arabidopsis thaliana* (L.) Heynh was used as the wild
31
32
33 type plant in this study. Sterile seeds were sown on Murashige and Skoog (MS) medium
34
35 that contained 3% (w/v) sucrose and 0.3% (w/v) gelrite (San-Ei Gen F.F.I., Inc.) in
36
37
38 plastic petri dishes, and then stratified for 2 days (d) at 4°C in the dark. Plants were
39
40
41 grown at 22°C under long day conditions (16 hours (hr) light/8 hr dark cycles or
42
43
44 continuous light) in a growth chamber. A T-DNA insertion mutant (*atnfxl1-1*) of
45
46
47
48 *AtNFXL1* (N501399) was obtained from the *Arabidopsis* Biological Resource Center,
49
50
51
52 Ohio State University, Columbus, Ohio. For trichothecene or defense-related molecule
53
54
55 treatment, *Arabidopsis* seeds were sown on MS agar medium containing the indicated
56
57
58
59
60

1
2
3
4
5
6
7 substance, and plants were continuously grown. Alternatively, *Arabidopsis* plants were
8
9
10 first grown on MS medium without treatment, and then transferred to MS medium
11
12
13 containing the indicated molecules. Additional details of each treatment are noted in the
14
15
16
17 text or figure legends.
18
19
20

21 22 23 24 **Generation of transgenic plants**

25
26
27 A region of the *AtNFXL1* promoter (-795 basepairs relative to the start site at +1) was
28
29
30 amplified by PCR using primers 1
31
32 (5'-GCGAAGCTTACTGGTTAGATTGGTTTAAG-3') and 2
33
34 (5'-GCGGGATCCATTCTGCCTTGACTCCACAAA-3'), and then introduced into the
35
36
37
38 *HindIII* and *BamHI* sites of pBI121. For complementation analysis, a *SacI* fragment of
39
40
41 the F14N23 BAC clone containing the promoter region and coding region of *AtNFXL1*
42
43
44
45 was introduced into the *SacI* site of pSMAH621. Plasmids were introduced into wild
46
47
48 type or *atnfxl1* mutant plants by *in planta* transformation, as previously described
49
50
51
52 (Asano *et al.*, 2004). Several independent transformants were obtained, and detailed
53
54
55
56
57
58 analysis was carried out on T2 and T3 plants.
59
60

Reverse transcription-polymerase chain reaction (RT-PCR) analysis

In a total volume of 20 μ l, cDNAs were synthesized from 1 μ g of total RNA using SuperScript III reverse transcriptase (Invitrogen) with a oligo(dT)₁₆ primer, and then 0.5 μ l of the cDNA was subsequently used for PCR analysis. All PCR reactions were performed in a total volume of 10 μ l, for 24-28 cycles under the following conditions: denaturation, 94°C, 30 seconds (s); annealing, 55°C, 30 s; extension, 72°C, 30 s. The following gene-specific primers were used: *AtNFXL1* 120-438, 5'-CCCATATGCCTCCTAATACAGATAGAAATTC-3' and 5'-ACGTCGACCTCAGGAGCATTATTTCTTCTATG-3'; *AtNFXL1* 2363-3568, 5'-CGCCATATGCATGTGGTTCGTATAACCGCTA-3' and 5'-GACGTCGACCTCACATACCTTCTCCCAGT-3'; *ACT2/8*, 5'-CATCACACTTTCTACAATGAGCT-3' and 5'-CGACCTTAATCTTCATGCTGC-3'.

Real time PCR analysis

Real time PCR was performed using the LightCycler Quick System 350S (Roche

1
2
3
4
5
6
7 Diagnostics K.K., Tokyo, Japan) with SYBR Premix Ex Taq (TAKARA BIO INC.,
8
9
10 Shiga, Japan). The PCR reaction contained 1 x SYBR Premix Ex Taq, 0.2 µM of each
11
12
13 primer, and the appropriate dilution of cDNA in a final volume of 20 µl. The following
14
15
16 PCR program was used: initial denaturation, 95°C, 10 s; 40 cycles of 95°C, 5 s and 60°C,
17
18
19 20 s with a temperature transition rate of 20°C/s; melting curve analysis, 95°C, 0 s, 65°C,
20
21
22 15 s, and an increase to 95°C with a temperature transition rate of 0.1°C/s. To generate a
23
24
25 standard curve, homologous standards were used as external standards in all
26
27
28 experiments. Template DNA was quantified using the second derivative maximum
29
30
31 methods of the LightCycler Software Ver.3.5 (Roche Diagnostics), then normalized to
32
33
34 *Actin2/8* mRNA. The following gene-specific primers were used: At5g25930, 5'-
35
36
37 ACATTGCTCCAGAATACGC-3' and 5'-CATCGCCTCAGTCGTG-3'; *WRKY15*,
38
39
40 5'-TGCTCGAAGAAAAGAAAGATAAAAC-3' and 5'-
41
42
43 AGTAACAATCAACATGGACG-3'; At5g41750,
44
45
46 5'-AAAGGAACAGGTACTGAATCT-3' and 5'-
47
48
49 TGTAGTAACCTAACAGGAGGTAT-3'; *Hsf21*, 5'-GCCAGCTTAACACATATGGT-3'
50
51
52 and 5'-TCTGATTATTCATTCTCACTCGT-3'; *EDS5*, 5'-GGTACATTGCTGGCGG-3'
53
54
55
56
57
58
59
60

1
2
3
4
5
6
7 and 5'-GTATGCCTCCAGGCGA-3'; At3g60420,
8
9
10 5'-AGATCAAGGTGGCTATTGAA-3' and 5'-CTCAAAGGCTTGTGCAG-3'; *MYB29*,
11
12
13 5'-TTCTCGCGCAACAAG-3' and 5'-GCTGGTTATCTCCGGTACA-3'; *Actin2/8*,
14
15
16 5'-GGTAACATTGTGCTCAGTGGTGG-3' and
17
18
19
20 5'-AACGACCTTAATCTTCATGCTGC-3'; *ICS1*, 5'-
21
22
23 ATGAGATTCAGCCTCGCTGT-3' and 5'-TGATGGATCTCCAATCGTCA-3'; *PR-1*,
24
25
26 5'-ATTACTTCATTAGTATGGCTTCT-3' and 5'-CTTGTCTGGCGTCTCC-3'. All kits
27
28
29
30
31 were used according to the manufacture's protocols.
32
33
34
35
36
37

38 **Microarray analysis**

39
40
41 Ten-day-old seedlings of wild type and *atnfxl1* mutant plants were grown on MS plates
42
43
44 and harvested after mock or 1 μ M T-2 toxin treatment for 24 hr. Samples for microarray
45
46
47 analysis were taken at the middle stage of the light period. Total RNA was prepared
48
49
50
51 from T-2 toxin-treated or untreated *Arabidopsis* shoots using a guanidine
52
53
54 hydrochloride–phenol-chloroform extraction method, as previously described
55
56
57
58 (Nishiuchi et al., 2006). The quality of RNA was assessed using the RNA 6000 Nano
59
60

1
2
3
4
5
6
7 LabChip Kit (Bioanalyzer 2100; Agilent Technologies, Inc.), then the microarray
8
9
10 experiment was carried out using the Agilent *Arabidopsis* 1 Oligo Microarray (Agilent
11
12
13 Technologies, Inc.), according to the Agilent 60-mer Oligo Microarray Processing
14
15
16 Protocol (Agilent Technologies, Inc.). Total RNA (5 μ g) from wild type and *atnfxl1*
17
18
19 mutant plants was used to prepare Cy3- and Cy5-labeled cDNAs, respectively, using a
20
21
22 Fluorescent Direct Labeling Kit (Agilent Technologies). The two different fluorescently
23
24
25 labeled cDNAs were combined and purified using an RNeasy RNA purification Kit
26
27
28 (Qiagen Inc.). Following hybridization and washing, arrays were scanned under
29
30
31 maximum laser intensity with both the Cy3 and Cy5 channels using an Agilent
32
33
34 microarray scanner (G2565BA; Agilent Technologies). Images were analyzed with
35
36
37 Feature Extraction Software (version 7.0; Agilent Technologies). Two independent
38
39
40 experiments were carried out using different plant samples to demonstrate the
41
42
43 reproducibility of the microarray analysis. Upregulated or downregulated genes were
44
45
46 designated as such if a 3-fold or greater change in expression relative to wild type plants
47
48
49 was observed. All changes in gene expression were statistically significant ($P < 0.01$).
50
51
52
53
54
55
56
57
58
59
60

SA measurement.

SA and SAG levels in mock- or T-2 toxin-treated samples were measured as described previously (Nakashita et al., 2002).

GUS assays

For GUS staining, plants were continuously treated with the indicated substance for 8 days. The *AtNFXL1 promoter::GUS* transformants were fixed in 90% acetone at -20°C, then incubated in a solution containing 0.5 mM $K_4[Fe(CN)_6]$, 0.5 mM $K_4[Fe(CN)_6] \cdot 3H_2O$, 1 mM EDTA, and 1 mM X-Gluc in 100 mM phosphate buffer (pH7.2) at 37°C for 2 hr. Samples were destained by a series of ethanol washes. For the fluorometric assay, 8-day-old plants were transferred to medium containing the indicated substance, incubated for 24 hr, and then subjected to quantification of GUS activity. The fluorometric assay of GUS activity was performed as previously described (Nishiuchi et al., 1995).

Bacterial Infection

1
2
3
4
5
6
7 The *Pst*DC3000 infection assay was performed as previously described (Yasuda *et al.*,
8
9
10 2003).

11 12 13 14 15 16 17 **Visualization of the GFP-AtNFXL1 fusion protein.**

18
19 The entire coding region of *AtNFXL1* was amplified from cDNA by PCR using the
20
21 following primers: 5'-CACCATGAGCTTTCAAGTCAGGCG-3' and
22
23 5'-TCACTCACATACCTTCTCCC-3'. The PCR fragment was inserted into the
24
25 pENTRTM/D-TOPO entry vector (Invitrogen Inc, Germany), then introduced into
26
27 pH7WGF2 (Karimi *et al.*, 2002). Protoplasts of *Arabidopsis* T87 suspension culture
28
29 cells were transiently transfected with the GFP-AtNFXL1 plasmid using the
30
31 polyethylene glycol (PEG) method (Abel and Theologis, 1994). GFP was visualized by
32
33 microscopy (BX-50; Olympus Optical, Tokyo) using a built-in BX-FLA epifluorescent
34
35 unit.
36
37
38
39
40
41
42
43
44
45

46 **Acknowledgement**

47
48
49 We thank Dr. Hiroaki Ichikawa for kindly providing the binary vector, pSMAH621
50
51
52
53 containing the hygromycin-resistance gene (*hpt*) as a selection marker.
54
55
56
57
58
59
60

References

- 1
2
3
4
5
6
7
8
9
10
11 **Abel, S. and Theologis, A.** (1994) Transient transformation of Arabidopsis leaf
12
13 protoplasts: a versatile experimental system to study gene expression. *Plant J.* **5**,
14
15
16
17 421-427.
18
19
20
21 **Asai, T., Tena, G., Plotnikova, J., Willmann, M.R., Chiu, W.L., Gomez-Gomez, L.,**
22
23
24 **Boller, T., Ausubel, F.M. and Sheen, J.** (2002) MAP kinase signalling cascade in
25
26
27 *Arabidopsis* innate immunity. *Nature* **415**, 977-983.
28
29
30
31 **Asano, T., Yoshioka, Y., Kurei, S., Sakamoto, W., Sodmergen and Machida, Y.**
32
33
34 (2004) A mutation of the *CRUMPLED LEAF* gene that encodes a protein localized in
35
36
37 the outer envelope membrane of plastids affects the pattern of cell division, cell
38
39
40
41 differentiation, and plastid division in *Arabidopsis*. *Plant J.* **38**, 448-459.
42
43
44
45 **Bai, G.H., Desjardins, A.E. and Plattner, R.D.** (2001) Deoxynivalenol-nonproducing
46
47
48 *Fusarium graminearum* causes initial infection, but does not cause disease spread in
49
50
51 wheat spikes. *Mycopathologia* **153**, 91-98.
52
53
54
55
56
57
58
59
60

- 1
2
3
4
5
6
7 **Baker, S.S., Wilhelm, K.S. and Thomashow, M.F.** (1994) The 5'-region of
8
9
10 *Arabidopsis thaliana cor15a* has *cis*-acting elements that confer cold-, drought- and
11
12
13
14 ABA-regulated gene expression. *Plant Mol. Biol.* **24**, 701-713.
15
16
17 **Bowling, S.A., Guo, A., Cao, H., Gordon, A.S., Klessig, D.F. and Dong, X.** (1994) A
18
19
20 mutation in *Arabidopsis* that leads to constitutive expression of systemic acquired
21
22
23
24 resistance. *Plant Cell* **6**, 1845-1857.
25
26
27 **Chen, C. and Chen, Z.** (2002) Potentiation of developmentally regulated plant defense
28
29
30 response by AtWRKY18, a pathogen-induced *Arabidopsis* transcription factor. *Plant*
31
32
33
34 *Physiol.* **129**, 706-716.
35
36
37 **Desjardins, A.E., Bai, G., Plattner, R.D. and Proctor, R.H.** (2000) Analysis of
38
39
40 aberrant virulence of *Gibberella zeae* following transformation-mediated
41
42
43
44 complementation of a trichothecene-deficient (*Tri5*) mutant. *Microbiology* **146**,
45
46
47
48 2059-2068.
49
50
51 **Dong, J., Chen, C. and Chen, Z.** (2003) Expression profiles of the *Arabidopsis*
52
53
54 WRKY gene superfamily during plant defense response. *Plant Mol. Biol.* **51**, 21-37.
55
56
57
58 **Eudes, F., Comeau, A., Rioux, S. and Collin, J.** (2001) Impact of trichothecenes on
59
60

1
2
3
4
5
6
7 *Fusarium* head blight [*Fusarium graminearum*] development in spring wheat
8
9
10 (*Triticum aestivum*). *Can. J. Plant Pathol.* **23**, 318-322.
11

12
13
14 **Eulgem, T., Rushton, P.J., Robatzek, S. and Somssich, I.E.** (2000) The WRKY
15
16
17 superfamily of plant transcription factors. *Trends Plant Sci.* **5**, 199-206.
18

19
20
21 **Gewin, L., Myers, H., Kiyono, T. and Galloway, A.D.** (2004) Identification of a novel
22
23
24 telomerase repressor that interacts with the human papillomavirus type-16 E6/E6-AP
25
26
27 complex. *Genes Dev.* **18**, 2269-2282.
28

29
30
31 **Kimura, M., Takahashi-Ando, N., Nishiuchi, T., Ohsato, S., Tokai, T., Ochiai, N.,**
32
33
34 **Fujimura, M., Kudo, T., Hamamoto, H. and Yamaguchi, I.** (2006) Molecular
35
36
37 biology and biotechnology for reduction of *Fusarium* mycotoxin contamination.
38
39
40
41 *Pestic. Biochem. and Physiol.* **86**, 117-123.
42

43
44
45 **Karimi, M., Inze, D. and Depicker, A.** (2002) Gateway vectors for
46
47
48 Agrobacterium-mediated plant transformation. *Trends Plant Sci.* **7**, 193-195.
49

50
51
52 **Kunz, J., Loeschmann, A., Deuter-Reinhard, M. and Hall, M.N.** (2000) FAP1, a
53
54
55 homologue of human transcription factor NF-X1, competes with rapamycin for
56
57
58 binding to FKBP12 in yeast. *Mol. Microbiol.* **37**, 1480-1493.
59
60

- 1
2
3
4
5
6
7 **Kurkela, S. and Franck, M.** (1990) Cloning and characterization of a cold- and
8
9
10 ABA-inducible *Arabidopsis* gene. *Plant Mol. Biol.* **15**, 137-144.
11
12
13
14 **Lang, V. and Palva, E.T.** (1992) The expression of a *rab*-related gene, *rab18*, is
15
16
17 induced by abscisic acid during the cold acclimation process of *Arabidopsis thaliana*
18
19
20 (L.) Heynh. *Plant Mol. Biol.* **20**, 951-962.
21
22
23
24 **Lisso, J., Altmann, T. and Mussig, C.** (2006) The *AtNFXL1* gene encodes a NF-X1
25
26
27 type zinc finger protein required for growth under salt stress. *FEBS Lett.* **580**,
28
29
30 4851-4856.
31
32
33
34 **Liu, Y., Schiff, M. and Dinesh-Kumar, S.P.** (2004) Involvement of MEK1 MAPKK,
35
36
37 NTF6 MAPK, WRKY/MYB transcription factors, *COII* and *CTR1* in *N*-mediated
38
39
40 resistance to tobacco mosaic virus. *Plant J.* **38**, 800-809.
41
42
43
44 **Lorick, K.L., Jensen, J.P., Fang, S., Ong, A.M., Hatakeyama, S. and Weissman,**
45
46
47 **A.M.** (1999) RING fingers mediate ubiquitin-conjugating enzyme (E2)-dependent
48
49
50 ubiquitination. *Proc. Natl. Acad. Sci.* **96**, 11364-11369.
51
52
53
54
55 **Masuda, D., Ishida, M., Yamaguchi, K., Yamaguchi, I., Kimura, M. and Nishiuchi,**
56
57
58 **T.** (2007) Phytotoxic effects of trichothecenes on the growth and morphology in
59
60

1
2
3
4
5
6
7 *Arabidopsis thaliana*. *J. Exp. Bot.* **58**, 1617-1626.

8
9
10 **Mauch-Mani, B. and Mauch, F.** (2005) The role of abscisic acid in plant-pathogen
11
12 interactions. *Curr. Opin. Plant Biol.* **8**, 409-414.

13
14
15
16
17 **Nawrath, C., Heck, S., Parinthewong, N. and Metraux, J.P.** (2002) EDS5, an
18
19 essential component of salicylic acid-dependent signaling for disease resistance in
20
21 *Arabidopsis*, is a member of the MATE transporter family. *Plant Cell* **14**, 275-286.

22
23
24
25
26
27 **Nishiuchi, T., Masuda, D., Nakashita, H., Ichimura, K., Shinozaki, K., Yoshida, S.,**
28
29
30 **Kimura, M., Yamaguchi, I. and Yamaguchi, K.** (2006) *Fusarium* phytotoxin
31
32 trichothecenes have an elicitor-like activity in *Arabidopsis thaliana*, but the activity
33
34 differed significantly among their molecular species. *Mol. Plant Microbe Interact.* **19**,
35
36
37
38
39
40
41 512-20.

42
43
44 **Nishiuchi, T., Nakamura, T., Abe, T., Kodama, H., Nishimura, M. and Iba, K.**
45
46 (1995) Tissue-specific and light-responsive regulation of the promoter region of the
47
48 *Arabidopsis thaliana* chloroplast ω -3 fatty acid desaturase gene (*FAD7*). *Plant Mol.*
49
50
51
52
53
54
55 *Biol.* **29**, 599-609.

1
2
3
4
5
6
7 **Robatzek, S. and Somssich, I.E.** (2002) Targets of AtWRKY6 regulation during plant
8
9
10 senescence and pathogen defense. *Genes Dev.* **16**, 1139-1149.
11

12
13 **Rogers, E.E., and Ausubel, F.M.** (1997) *Arabidopsis* enhanced disease susceptibility
14
15
16
17 mutants exhibit enhanced susceptibility to several bacterial pathogens and alterations
18
19
20 in *PR-1* gene expression. *Plant Cell* **9**, 305-316.
21

22
23 **Serrano, M. and Guzman, P.** (2004) Isolation and gene expression analysis of
24
25
26
27 *Arabidopsis thaliana* mutants with constitutive expression of *ATL2*, an early
28
29
30 elicitor-response RING-H2 zinc-finger gene. *Genetics* **167**, 919-29.
31

32
33 **Shifrin, V.I. and Anderson, P.** (1999) Trichothecene mycotoxins trigger a ribotoxic
34
35
36
37 stress response that activates c-Jun N-terminal kinase and p38 mitogen-activated
38
39
40 protein kinase and induces apoptosis. *J. Biol. Chem.* **274**, 13985-13992.
41

42
43
44 **Song, Z., Krishna, S., Thanos, D., Strominger, J.L. and Ono, S.J.** (1994) A novel
45
46
47
48 cysteine-rich sequence-specific DNA-binding protein interacts with the conserved
49
50
51 X-box motif of the human major histocompatibility complex class II genes via a
52
53
54 repeated Cys-His domain and functions as a transcriptional repressor. *J. Exp. Med.*
55
56
57
58 **180**, 1763-1774.
59
60

1
2
3
4
5
6
7 **Stroumbakis, N.D., Li, Z. and Tolias, P.P.** (1996) A homolog of human transcription
8
9
10 factor NF-X1 encoded by the *Drosophila shuttle craft* gene is required in the
11
12
13 embryonic central nervous system. *Mol. Cell Biol.* **16**, 192-201.
14
15

16
17 **Sudakin, D.L.** (2003) Trichothecenes in the environment: relevance to human health.
18
19
20 *Toxicol. Lett.* **143**. 97-107.
21
22

23
24 **Takai, R., Matsuda, N., Nakano, A., Hasegawa, K., Akimoto, C., Shibuya, N. and**
25
26
27 **Minami, E.** (2002) EL5, a rice *N*-acetylchitooligosaccharide elicitor-responsive
28
29
30 RING-H2 finger protein, is a ubiquitin ligase which functions *in vitro* in co-operation
31
32
33 with an elicitor-responsive ubiquitin-conjugating enzyme, *OsUBC5b*. *Plant J.* **30**,
34
35
36
37
38 447-455.
39

40
41 **Ulker, B. and Somssich, I.E.** (2004) WRKY transcription factors: from DNA binding
42
43
44 towards biological function. *Curr. Opin. Plant Biol.* **7**, 491-498.
45
46

47
48 **Urban, M., Daniels, S., Mott, E. and Hammond-Kosack, K.** (2002) *Arabidopsis* is
49
50
51 susceptible to the cereal ear blight fungal pathogens *Fusarium graminearum* and
52
53
54 *Fusarium culmorum*. *Plant J.* **32**, 961-973.
55
56
57
58
59
60

1
2
3
4
5
6
7 **Ward, T.J., Bielawski, J.P., Kistler, H.C., Sullivan, E. and O'Donnell, K. (2002)**
8

9
10 Ancestral polymorphism and adaptive evolution in the trichothecene mycotoxin gene
11
12 cluster of phytopathogenic *Fusarium*. *Proc. Natl. Acad. Sci.* **99**, 9278-9283.
13
14
15

16
17 **Wildermuth, M.C., Dewdney, J., Wu, G. and Ausubel, F.M. (2001) Isochorismate**
18

19
20 synthase is required to synthesize salicylic acid for plant defence. *Nature* **414**,
21
22 562-565.
23
24
25

26
27 **Yasuda, M., Nakashita, H., Hasegawa, S., Nishioka, M., Arai, Y., Uramoto, M.,**
28

29
30
31 **Yamaguchi, I. and Yoshida, S. (2003) *N*-cyanomethyl-2-chloroisonicotinamide**
32
33 induces systemic acquired resistance in *Arabidopsis* without salicylic acid
34
35 accumulation. *Biosci. Biotechnol. Biochem.* **67**, 322-328.
36
37
38
39
40
41
42
43
44
45
46
47
48
49
50
51
52
53
54
55
56
57
58
59
60

Table 1. Upregulated genes in 1 μM T-2 toxin-treated *atnfx1* mutant plants compared to T-2 toxin-treated wild type p

Functional category	Accession	FC	P value*	FC	P value*
Cellular Communication / Signal Transduction*					
protein kinase					
	A1503920 serine threonine kinase-like protein	7.8	1.9E-05	6.0	3.5E-05
	A1539670 serine threonine kinase-like protein	6.6	3.6E-05	4.9	1.4E-04
	A1539680 protein kinase-like protein	4.8	3.8E-04	5.3	1.7E-03
	A1411890 NAC-like protein kinase	5.1	1.2E-04	4.8	1.6E-04
	A1423200 similar to serine/threonine/tyrosine-specific protein	4.7	2.0E-04	3.4	1.7E-03
	A1506880 serine threonine kinase-like protein	3.4	1.3E-03	4.2	3.6E-04
	A1507080 protein kinase-like protein (MAPKKK19)	4.2	3.3E-04	3.1	5.8E-03
	A1506560 protein kinase-like protein	3.5	1.2E-03	3.3	6.4E-03
receptor-like protein kinase					
	A1519470 putative receptor-like protein kinase	6.3	4.2E-05	6.1	4.9E-05
	A1302500 similar to receptor-like serine/threonine protein kinase	3.5	1.0E-03	5.3	9.8E-05
	A1404500 receptor-like protein kinase-like	5.7	7.6E-05	3.1	2.3E-03
A1503930 receptor protein kinase-like protein					
	A1347480 receptor protein kinase-like protein	4.2	3.6E-04	3.8	6.1E-04
	A1347480 receptor protein kinase-like protein	4.6	2.0E-04	3.3	1.4E-03
	A1406850 receptor protein kinase-like protein	3.3	1.5E-03	4.2	3.6E-04
	A1509020 S-receptor kinase homolog 2 precursor	3.6	9.6E-04	3.7	1.3E-03
	A1423280 similar to disease resistance protein kinase Pto	3.6	8.9E-04	3.6	1.9E-03
	A1503000 serine threonine-specific protein kinase-like (RLK1)	3.9	5.6E-04	3.1	2.2E-03
calcium-binding protein					
	A1291100 putative calcium-binding protein (TCH3)	6.8	3.2E-05	7.5	2.1E-05
	A1417680 hypotheical protein, EF-hand calcium-binding domain	6.0	7.3E-05	6.0	1.6E-04
	A1407280 calcium-binding protein-like	3.4	1.4E-03	9.5	9.8E-06
	A1542380 putative caltractin	5.9	5.6E-05	4.2	3.2E-04
	A1505440 putative protein, EF-hand calcium-binding domain	5.0	1.3E-04	4.9	1.7E-04
calmodulin-related protein					
	A1301830 calmodulin-binding-like protein	5.6	7.2E-05	6.0	5.2E-05
	A1513200 calmodulin-like protein	5.8	6.0E-05	5.7	6.5E-05
	A1423150 calmodulin-like protein	4.1	4.2E-04	3.2	2.2E-03
	A1501560 calmodulin, putative	3.1	2.5E-03	4.1	4.2E-04
others					
	A1497010 caltractin-like protein	4.1	4.4E-04	4.1	5.9E-04
	A1493890 small GTP-binding protein-like	3.0	3.0E-03	4.1	7.3E-04
Transcription					
WRKY family protein					
A1293320 putative WRKY-type DNA-binding protein (WRKY15)					
	A1513080 WRKY-like protein (WRKY75)	6.5	3.8E-05	3.3	1.7E-03
	A1423810 similar to WRKY transcription factor AR411 (WRKY53)	4.0	4.4E-04	4.4	2.9E-04
	A1504820 similar to WRKY-type DNA binding protein (WRKY48)	3.4	1.4E-03	4.7	2.2E-04
	A1293220 putative WRKY-type DNA binding protein (WRKY25)	3.4	1.2E-03	4.4	2.9E-04
	A1162300 transcription factor WRKY6	4.5	2.4E-04	3.2	2.1E-03
	A1502270 WRKY transcription factor 36 (WRKY36)	3.2	2.2E-03	3.3	3.1E-03
	A1503170 WRKY transcription factor 50 (WRKY50)	3.1	2.5E-03	3.2	2.6E-03
NAC family protein					
	A1502280 NAC-domain protein-like (ANAC096)	3.3	1.7E-03	10.1	1.4E-05
	A12917040 NAM (no apical meristem)-like protein (ANAC036)	3.5	1.0E-03	4.0	4.8E-04
others					
	A1127730 salt-tolerance zinc finger protein (Zat10)	5.7	7.0E-05	6.3	4.3E-05
	A1505820 zinc finger protein Zat12	6.0	5.3E-05	5.5	7.7E-05
	A1305670 SigA binding protein	4.5	2.2E-04	5.7	6.9E-05
	A1294600 scarceow-like protein	3.2	1.9E-03	4.1	8.0E-04
	A1161850 putative myb transcription factor (MYB51)	3.7	1.0E-03	3.2	2.4E-03
	A1418880 heat shock transcription factor 21 (AHSF21)	3.4	1.2E-03	3.2	1.9E-03
	A1501010 putative protein	3.1	1.5E-03	3.3	1.6E-03
	A1168840 putative DNA-binding protein (RAV2-like)	3.3	1.6E-03	3.1	2.3E-03
Defence Stress and Detoxification					
disease resistance protein					
A1504170 disease resistance protein-like					
	A1107630 disease resistance protein RPP1-WsB, putative	5.9	5.7E-05	6.0	5.2E-05
	A1501740 disease resistance protein-like	4.3	1.5E-04	4.4	2.7E-04
	A1172900 virus resistance protein, putative	3.8	6.5E-04	3.9	5.1E-04
	A1403300 similar to NBS/LRR disease resistance protein (RFL1)	3.5	1.1E-03	3.8	6.4E-04
glutathione S-transferase					
	A1171710 putative glutathione transferase	6.2	4.5E-05	6.0	5.1E-05
	A12947730 glutathione S-transferase (GST6)	3.4	1.4E-03	3.4	1.3E-03
others					
	A1502780 putative protein, similar to In2	7.6	2.1E-05	5.7	7.4E-05
	A1203980 similar to harpin-induced protein hri1 from tobacco	6.1	5.0E-05	5.0	1.3E-04
	A1414630 germ precursor oxidase oxidase	5.1	1.2E-04	3.1	2.2E-03
Cellular Transport and Transport Mechanisms					
ABC transporter					
	A1115520 ABC transporter, putative	7.2	2.5E-05	3.3	1.4E-03
	A12947000 putative ABC transporter	3.3	1.5E-03	4.0	4.4E-04
calcium-ATPase					
	A1306380 Ca ²⁺ -transporting ATPase-like protein	4.1	4.0E-04	3.7	7.0E-04
	A13022910 calmodulin-stimulated calcium-ATPase, putative	5.3	9.4E-05	4.6	2.0E-04
others					
	A1421880 peptide transporter-like protein	3.3	1.6E-03	9.5	1.1E-05
	A1426180 amino acid permease-like protein	5.4	8.9E-05	5.2	1.1E-04
	A12913810 putative aspartate aminotransferase	3.2	1.6E-03	4.7	8.0E-04
	A1502840 hexose transporter-like protein	4.2	3.4E-04	3.9	5.0E-04
	A1302400 syntaxin-like protein synt4	3.6	9.2E-04	4.1	3.8E-04
	A1501900 copine-like protein copine	3.1	2.4E-03	4.6	2.1E-04
	A15040780 amino acid permease	3.7	6.7E-04	3.4	1.2E-03
	A1108930 putative sugar transporter (ERD6)	3.1	2.6E-03	4.0	4.3E-04
Metabolism					
UDP-glucose glucosyltransferase					
	A1124200 UDP-glucose glucosyltransferase, putative	6.3	4.6E-05	3.1	2.3E-03
	A1294360 putative glucosyltransferase	4.0	4.7E-04	3.6	9.5E-04
	A1292010 putative glucosyltransferase	4.1	4.1E-04	3.5	1.1E-03
	A1105550 UDP-glucosyltransferase-3-acetate beta-D-	4.1	4.0E-04	4.1	2.1E-03
	A1404131 glucosyltransferase-like protein	3.3	1.6E-03	3.9	5.6E-04
cytochrome P450 family					
	A1503830 putative cytochrome P450	9.8	9.1E-06	4.5	2.9E-04
	A1504540 cytochrome P450	3.7	9.3E-04	7.3	7.9E-05
	A1403730 cytochrome P450-like protein	4.4	2.4E-04	3.9	5.4E-04
FAD-linked oxidoreductase family					
	A1504430 berberine bridge enzyme	4.3	2.9E-04	4.9	2.0E-04
	A1420830 reticuline oxidase-like protein	4.3	3.1E-04	4.4	2.6E-04
	A1403960 berberine bridge enzyme-like protein	3.7	7.0E-04	4.3	3.1E-04
flavonone 3-hydroxylase-like protein					
	A1504530 flavonone 3-hydroxylase-like protein	4.8	1.5E-04	4.3	3.0E-04
	A1301910 oxidase like protein	3.5	1.0E-03	3.1	2.1E-03
others					
	A1302600 predicted GPI-anchored protein	8.1	1.0E-05	4.5	2.2E-04
	A1403810 xyloglucan endo-1,4-beta-D-glucanase (XTR-6)	4.9	1.9E-04	4.7	3.8E-05
	A15042830 N-hydroxyoxindole benzoylesterase-like protein	5.6	7.4E-05	5.4	9.4E-05
	A1292680 similar to latex allergen from Hevea brasiliensis	6.2	4.5E-05	4.7	1.7E-04
	A1511730 glutamate decarboxylase 1 (GAD1) (sp Q4291)	5.0	1.2E-04	4.1	1.1E-04
	A1503800 InE protein-like	5.1	1.2E-04	4.1	3.7E-04
	A1501830 nucleokinase 1	3.6	9.8E-04	5.2	1.1E-04
	A1403830 putative L-ascorbate oxidase	3.6	9.5E-04	4.7	1.9E-04
	A1403070 putative phosphoribosylanthranilate transferase	4.7	1.7E-04	3.3	1.5E-03
	A1401700 putative chitinase	3.8	6.0E-04	3.6	9.2E-04
	A15038710 protein oxidase, mitochondrial precursor-like protein	3.3	1.7E-03	3.9	1.3E-03
	A1174710 isochorismate synthase (icsl)	3.7	7.2E-04	3.3	1.5E-03
	A1519440 cinnamyl-alcohol dehydrogenase-like protein	3.4	1.2E-03	3.1	2.3E-03
DNA Synthesis and Processing					
	A1293020 putative alanine acetyl transferase	3.3	1.6E-03	4.8	1.6E-04
	A1501100 putative protein	3.6	1.3E-03	4.3	3.3E-03
Protein Fate					
	A1506800 putative protein, similar to GFP5	4.1	4.1E-04	8.6	1.5E-05
	A1305030 BCS1 protein-like protein	5.2	1.1E-04	5.7	6.8E-05
Cellular Structural Organization					
	A1504310 arabinoxylan-protein (gp AAC77823.1)	5.2	1.1E-04	4.6	2.0E-04
Enzyme					
	A1102350 oxidase, putative	7.8	1.9E-05	3.7	7.1E-04
Protein Synthesis					
	A1416680 RNA helicase	4.4	2.9E-04	3.7	1.7E-03
Unclassified Protein					
	A13060420 putative protein	11.7	5.7E-06	14.1	3.9E-06
	A1504990 GDLSL-motif lipase hydrolase-like protein	12.0	6.3E-06	9.2	5.5E-05
	A1191620 unknown protein	7.1	2.7E-05	6.8	3.6E-05
	A1291600 class 1 non-symbiotic hemoglobin (AHB1)	5.6	7.5E-05	7.8	1.8E-05
	A1511140 putative protein, similar to pEARL1.4	5.8	6.1E-05	5.4	9.0E-05
	A1401670 predicted protein of unknown function	3.7	7.1E-04	6.9	2.9E-05
	A1165500 unknown protein	4.4	2.6E-04	5.1	1.1E-04
	A1129290 unknown protein	4.4	2.6E-04	4.6	2.0E-04
	A15049410 isoantigen-like channel protein-like (AGLR1.3)	5.8	6.6E-05	3.4	2.2E-03
	A15027420 RING-H2 zinc finger protein-like	4.7	1.9E-04	4.2	7.0E-04
	A1314225 unknown protein	5.3	2.9E-04	3.5	3.9E-03
	A1150800 hypotheical protein	6.1	5.3E-05	3.0	2.9E-03
	A14022530 putative protein	4.3	2.9E-04	4.0	4.5E-04
	A1504970 putative protein	3.4	1.2E-03	5.0	2.0E-04
	A1504900 ligand-gated ion channel protein-like; glutamate receptor-	5.0	1.3E-04	3.2	2.1E-03
	A1155450 hypotheical protein	3.6	8.5E-04	4.3	2.9E-04
	A1404020 putative protein, similar to myosin heavy chain	3.5	1.4E-03	4.5	9.9E-04
	A1503230 putative protein	3.8	8.4E-04	3.9	6.9E-03
	A1294600 polygalacturonase inhibiting protein 1; PGIP1 (gp	3.4	1.2E-03	3.8	6.1E-04
	A11016420 hypotheical protein	3.9	5.9E-04	3.1	2.2E-03
	A1412720 growth factor like protein	3.8	6.0E-04	3.1	2.6E-03
	A1123710 unknown protein	3.5	1.0E-03	3.3	1.7E-03
	A1193840 putative RING zinc finger protein	3.7	7.5E-04	3.1	2.6E-03
	A1504000 3',5'-bisphosphate nucleotidase (GAL2)	3.0	3.2E-03	3.7	1.9E-03
	A14038540 monoxygenase 2 (MO2)	3.0	2.7E-03	3.7	8.3E-04
	A14024180 putative protein	3.1	2.5E-03	3.5	1.0E-03
	A1502190 putative protein, similar to PPMC3	3.0	2.8E-03	3.3	3.2E-03
	A15028210 putative protein	3.1	2.3E-03	3.0	2.9E-03

Ten-day-old seedlings of wild type and *atnfx1* mutant plants were grown MS plates and harvested after 1 μM T-2 toxin treatment for 24 h.

Genes in bold-face expression was verified by real time RT-PCR (see Table 3).

*Classification of functional category was based on information from the Munich Information Center for Protein Sequence (MIPS).

†Upregulated genes were designated as such based on a 3-fold or greater change (FC) in the normalized signal between T-2 toxin-treated *atnfx1* m

‡All of these changes in gene expression were statistically significant, with at P<0.01.

Table 2. Downregulated genes in the T-2 toxin-treated *atnfx11* mutant plants compared to T-2 toxin-treated w

AGI code	Descriptions	exp.1		exp.2	
		FC ^a	P value ^b	FC	P value
At4g19170	neoxanthin cleavage enzyme-like protein	0.164	5.6E-03	0.073	2.0E-03
At4g16830	nuclear antigen homolog	0.111	3.3E-03	0.164	5.7E-03
At5g50950	fumarate hydratase	0.150	4.8E-03	0.137	4.3E-03
At5g23010	2-isopropylmalate synthase-like	0.206	8.7E-03	0.090	2.5E-03
At4g13770	cytochrome P450 monooxygenase (CYP83A1)	0.193	7.7E-03	0.111	3.2E-03
At5g07690	myb family transcription factor (MYB29)	0.200	8.7E-03	0.116	3.6E-03
At1g14250	nucleoside phosphatase family protein / GDA1/CD39 family protein	0.200	8.3E-03	0.128	4.0E-03
At5g03760	glycosyl transferase family 2 protein	0.161	5.8E-03	0.174	7.3E-03
At4g21650	subtilisin proteinase - like	0.206	8.9E-03	0.151	5.0E-03
At3g27690	chlorophyll A-B binding protein (LHCB2:4)	0.196	7.9E-03	0.164	5.6E-03
At5g12250	tubulin beta-6 chain	0.189	7.3E-03	0.186	7.2E-03
At4g21960	peroxidase 42 (PER42)	0.217	9.8E-03	0.199	8.1E-03

Ten-day-old seedlings of wild type and *atnfx11* mutant plants were grown MS plates and harvested after mock or 1 μ M T-2 toxin treatment for 7 days. The expression of MYB29 (bold-face) was verified by real time RT-PCR analysis (see Table 3).

^aDownregulated genes were designated as such based on a 3-fold or greater change in the normalized signal of T-2 toxin-treated *atnfx11* n

^bAll of these changes in gene expression were statistically significant, with $P < 0.01$.

CONFIDENTIAL

Table 3. Validation of microarray results in the 1 μ M T-2 toxin-treated plants by real time PCR.

Fold change (<i>atnfx11</i> mutant vs wild type)			
AGI code	Microarray ^a	real time PCR ^b	Description
Upregulated Genes			
At5g25930	4.00	11.6 \pm 1.39	receptor protein kinase-like protein
At2g23320	5.17	4.87 \pm 0.26	putative WRKY-type DNA-binding protein (WRKY15)
At4g18880	3.30	5.21 \pm 0.68	heat shock transcription factor 21 (AtHSF21)
At5g41750	5.97	12.08 \pm 1.56	disease resistance protein-like
At4g39030	3.76	7.52 \pm 1.04	enhanced disease susceptibility 5 gene (EDS5)
At3g60420	12.84	11.56 \pm 2.16	putative protein
Downregulated genes			
At5g07690	0.15	0.12 \pm 0.02	Myb family transcription factor (MYB29)

Ten-day-old seedlings of wild type and *atnfx11* mutant were grown MS plate and harvested after 1 μ M T-2 toxin treat

^aFold change in microarray results is the average value of two arrays.

^bFold change in real time PCR is an average value of four independent biological sample sets.

CONFIDENTIAL

Figure legends

Figure 1. An *atnfxl1* mutant (*atnfxl1-1*) is hypersensitive to type A trichothecenes. (a) Schematic diagram of *AtNFXL1* in *Arabidopsis thaliana*. Boxes indicate exons. The organization of the exon-intron boundary was predicted by the nucleotide sequence of the full length cDNA, and is identical to our results. The T-DNA insertion site is indicated by a triangle. Two different regions (basepairs 120-438 and 2368-3568) of *AtNFXL1* for RT-PCR analysis is indicated by thick lines. (b) A truncated transcript of *AtNFXL1* was observed in the *atnfxl1-1* mutant. Ten-day-old seedlings of wild type and *atnfxl1-1* mutant plants were grown on MS plates and harvested after mock treatment, or 1 μ M T-2 toxin treatment for 24 hr. Total RNA was prepared from the seedlings and used for RT-PCR analysis. Two different regions (basepairs 120-438 and 2368-3568) of *AtNFXL1* were amplified by specific primer sets. *Actin2/8* was used as a loading control. (c) Representative photographs of wild type, *atnfxl1*, and complementation plant lines that were mock-treated (upper row), or treated with 0.1 μ M T-2 toxin (lower row). Sterile seeds were sown on MS medium with or without 0.1 μ M T-2 toxin, and then stratified for 2 d at 4°C in the dark. Plants were grown for 8 days in a growth chamber,

1
2
3
4
5
6
7 and then photographed. Scale bars = 1 cm. (d) The fresh weight of each plant is
8
9
10 expressed relative (%) to mock-treated wild type. Plants were treated with 0.1 μ M T-2
11
12
13 toxin or 10 μ M DON without trichothecenes, as stated above.
14
15
16
17 *atnfxl1:PAtnFXL1::AtNFXL1* (line #5) refers to an *atnfxl1* mutant carrying an *AtNFXL1*
18
19
20 *promoter::AtNFXL1* gene fusion. Data is representative of two independent experiments.
21
22
23
24 *, $P < 0.01$, based on the Student's *t*-test. Similar results were obtained in other six
25
26
27 independent complementation lines.
28
29
30
31
32
33

34 Figure 2. *AtNFXL1* is involved in SA biosynthesis and expression of SA-related genes.
35
36
37 Eight-day-old plants were either mock-treated or treated with 1 μ M T-2 toxin for 24 hr
38
39
40 and then subjected to Real time PCR analysis (a) or SA quantification (b-c). (a) Real
41
42
43 time PCR analysis of *PR-1* and *ICS1* of *atnfxl1* mutant and wild type plants. Total RNA
44
45
46 was isolated from each sample and then subjected to Real time PCR analysis. The levels
47
48
49 of mRNA were determined by real-time RT-PCR, and normalized with that of *Actin2/8*.
50
51
52
53
54
55 Expression levels are relative to that of mock-treated wild type samples. Data is the
56
57
58 average of three independent samples. Error bars indicate the standard deviation. (b-c)
59
60

1
2
3
4
5
6
7 Enhanced accumulation of SA in T-2 toxin-treated *atnfxl1* mutant plants. (b) Free and
8
9
10 (c) total SA levels were quantified by high-performance liquid chromatography (data
11
12
13
14 represents the means \pm standard deviation, n=4).
15
16
17
18
19

20
21 Figure 3. GUS staining and quantification of GUS activity in *AtNFXL1 promoter::GUS*
22
23 stable transformants in response to elicitor, phytohormone, or trichothecene treatment.
24
25 GUS staining of mock- (a), T-2 toxin- (b) or SA-treated 8 day old plants (c). Sterile
26
27 seeds were sown on MS agar medium with 0.1 μ M T-2 or 100 μ M SA, and then
28
29 stratified for 2 d at 4°C in the dark. Plants were grown for 8 days in a growth chamber,
30
31 and then subjected to GUS staining. Scale bars = 1 mm. (d) Quantification of GUS
32
33 activity in *AtNFXL1 promoter::GUS* stable transformants treated with the indicated
34
35 substances. Plants were grown for 8 days on MS agar medium in a growth chamber, and
36
37 then either mock-treated or treated with the indicated substance for 24 hr and used for
38
39 quantitative GUS assays. GUS activity in treated samples relative to mock-treated
40
41 samples was measured using a fluorometric GUS assays (n=4). Data is representative of
42
43 two independent experiments.
44
45
46
47
48
49
50
51
52
53
54
55
56
57
58
59
60

1
2
3
4
5
6
7
8
9
10 Figure 4. Reduced susceptibility of *atnfxl1* mutant plants to the compatible pathogen *Pst*
11 DC3000. (a) Leaves of *atnfxl1* mutant (closed circles) and wild type (open circles)
12
13
14 plants were collected 0, 1, 2 and 4 days post-inoculation and homogenized in 10 mM
15
16
17 MgCl₂. The number of colony-forming units (CFU) was estimated by growth on
18
19
20 nutrient broth agar plates after the appropriate dilution. Data represents the averages ±
21
22
23 standard deviation (n=6). A significant difference between wild type and *atnfxl1* mutant
24
25
26 plants was observed in the number of CFU/g fresh weight (p<0.05, ANOVA). Data is
27
28
29 representative of two independent experiments. (b) Complementation analysis of the
30
31
32 reduced susceptibility to *Pst*DC3000 in an *atnfxl1* mutant. Leaves of wild type, *atnfxl1*,
33
34
35 and complementation plant line were collected 2 days post-inoculation. Data represents
36
37
38 the averages ± standard deviation (n=6). A significant difference between the number of
39
40
41 CFU/g fresh weight of *atnfxl1* mutant plants and wild type/complementation line #4
42
43
44 plants was observed (p<0.05, ANOVA). Similar results were obtained in
45
46
47
48
49
50
51
52
53
54
55
56
57
58
59
60
complementation lines #1 and #3.

1
2
3
4
5
6
7 Figure 5. Model of opposing functions of *AtNFXL1* in biotic and abiotic stress response.
8
9

10 Biotic stress often causes accumulation of elicitors and/or SA in host plants. SA and
11
12
13
14
15
16
17
18
19
20
21
22
23
24
25
26
27
28
29
30
31
32
33
34
35
36
37
38
39
40
41
42
43
44
45
46
47
48
49
50
51
52
53
54
55
56
57
58
59
60
AtNFXL1 functions as a negative regulator of defense-related genes via an
SA-dependent signaling pathway, which resulting in reduced susceptibility to a virulent
pathogen, *Pst* DC3000 in the *atnfxl1* mutant. Abiotic stress such as salt and osmotic
stress also induces the expression of *AtNFXL1* (Lisso *et al.*, 2006). *AtNFXL1* functions
as a positive regulator of salt-responsive genes (Lisso *et al.*, 2006). The *atnfxl1* mutant
exhibited a reduced survival rate under salt stress (Lisso *et al.*, 2006).

Supplemental Figure 1. *AtNFXL1* belongs to the NF-X1 family of proteins.

(a) Schematic diagram of *AtNFXL1* in *Arabidopsis thaliana* (Accession no. AAD32867) and comparison of *AtNFXL1* with the following homologues: *OsNF-X1*, *Oryza sativa* (Accession no. BAD46154); *NF-X1*, *Homo sapiens* (Accession no. NP_002495); *STC*, *Drosophila melanogaster* (Accession no. NP_476599); *Fap1*,

1
2
3
4
5
6
7 *Saccharomyces cerevisiae* (Accession no. NP_014375). The purple regions indicate the
8
9
10 NLS; red and blue indicate the RING-CH finger domain and the nine NF-X1-type Zn
11
12
13
14
15
16
17
18
19
20
21
22
23
24
25
26
27
28
29
30
31
32
33
34
35
36
37
38
39
40
41
42
43
44
45
46
47
48
49
50
51
52
53
54
55
56
57
58
59
60

(b) A rooted maximum-likelihood phylogenetic tree of AtNFXL1 and AtNFXL1 homologues. DrNF-X1, *Danio rerio* (Accession no. XP_690559); MmNF-X1, *Mus musculus* (Accession no. AAF34700); CeNF-X1, *Caenorhabditis elegans* (Accession no. NP_498394); and SpNF-X1, *Schizosaccharomyces pombe* (Accession no. CAA21417).

(c) Alignment of the amino acid sequences of the nine AtNFXL1-type Zn finger domains. The number to the left of each repeat indicates its position in the AtNFXL1 protein sequence. The consensus sequence for the Zn finger repeat is shown above the sequences, and is based on matches in seven of the nine aligned sequences.

Supplemental Figure 2. Subcellular localization of GFP-AtNFXL1 and GFP proteins in *Arabidopsis* cells. Protoplasts of *Arabidopsis* T87 suspension culture cells were transfected using the polyethylene glycol (PEG) method. GFP-AtNFXL1 fusion protein localized to the nucleus of *Arabidopsis* cells (a-c). In contrast, GFP localized to the

1
2
3
4
5
6
7 cytosol (d-f). GFP fluorescence was visualized in using a fluorescence microscope.
8
9
10
11
12
13
14
15
16
17
18
19
20
21
22
23
24
25
26
27
28
29
30
31
32
33
34
35
36
37
38
39
40
41
42
43
44
45
46
47
48
49
50
51
52
53
54
55
56
57
58
59
60

CONFIDENTIAL

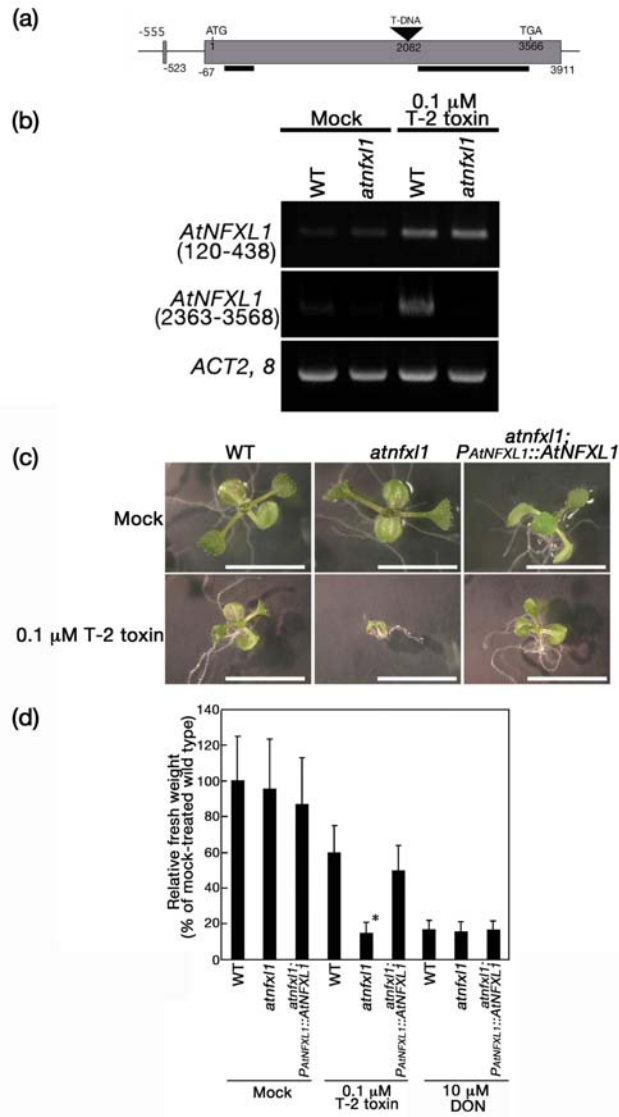


Figure 1

111x213mm (400 x 400 DPI)

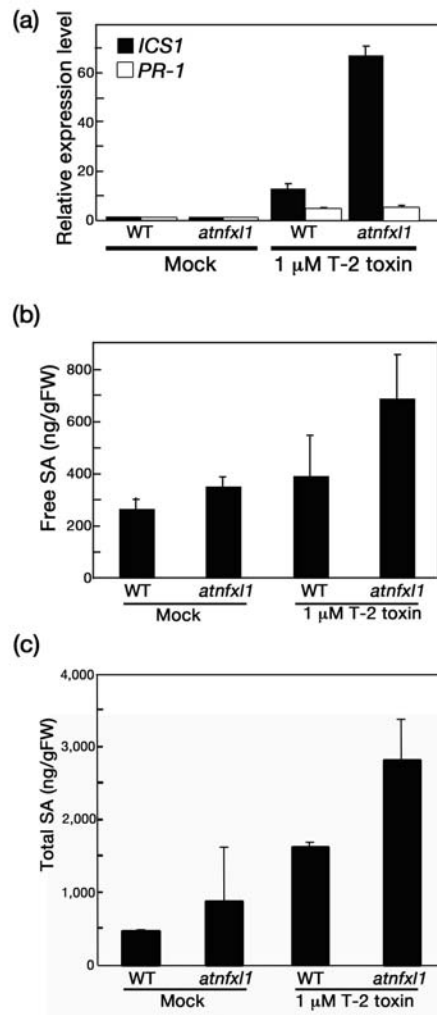
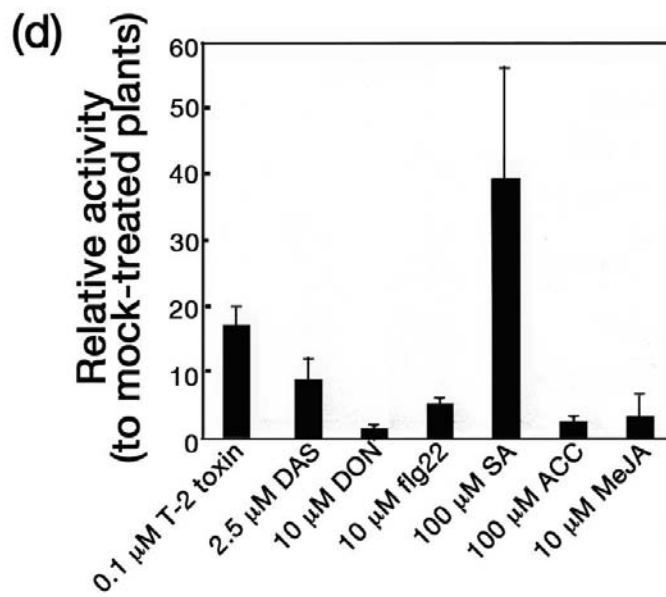
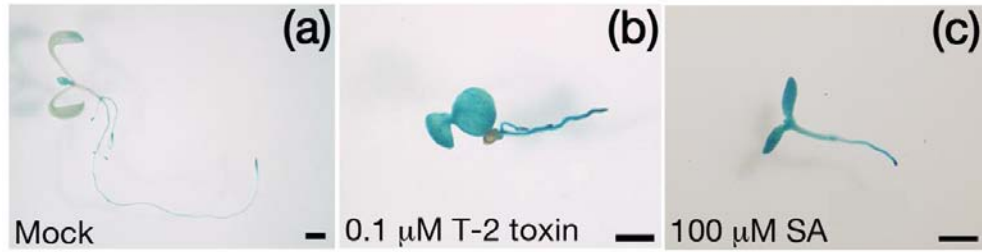


Figure 2

100x210mm (400 x 400 DPI)



39
40
41
42

Figure 3

43
44
45
46
47
48
49
50
51
52
53
54
55
56
57
58
59
60

80x82mm (400 x 400 DPI)

1
2
3
4
5
6
7
8
9
10
11
12
13
14
15
16
17
18
19
20
21
22
23
24
25
26
27
28
29
30
31
32
33
34
35
36
37
38
39
40
41
42
43
44
45
46
47
48
49
50
51
52
53
54
55
56
57
58
59
60

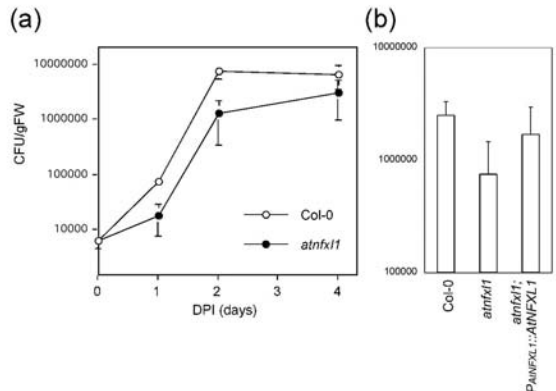


Figure 4

AL

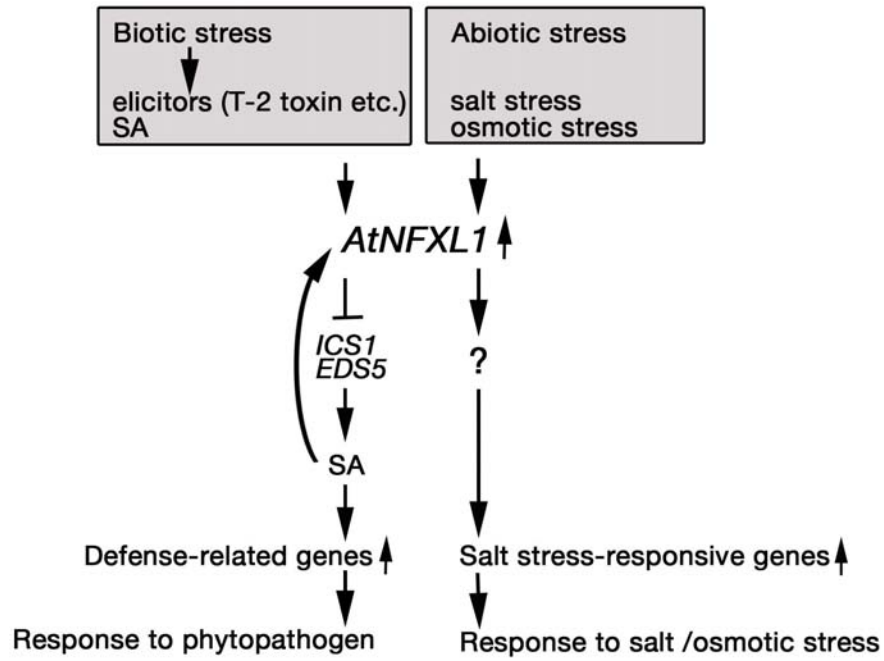


Figure 5

120x109mm (400 x 400 DPI)